

PROPAGATION CHARACTERISTICS OF A VARIANT OF DISC-LOADED CIRCULAR WAVEGUIDE

V. Kesari¹ and J. P. Keshari^{2, *}

¹Microwave Tube Research and Development Centre, Bangalore, India

²Galgotias College of Engineering and Technology, Greater Noida, India

Abstract—The shaping of dispersion characteristics in a variant of disc-loaded circular waveguide was studied through electromagnetic analysis for assessing the structure for wideband coalescence of the beam- and waveguide-mode dispersion characteristics that entails the wideband gyro-travelling-wave tube (gyro-TWT) performance. In this variant of disc-loaded circular waveguide, the alternate disc-hole radii were varying, however, the structure was periodic. The structure periodicity coupled with Floquet's theorem and field-matching technique resulted into the dispersion relation of the infinitely long structure. A numerical code was developed to solve the dispersion relation, and the dispersion characteristics of the structure were analyzed for the azimuthally symmetric TE-modes. The effects of structure parameters were studied for getting a straight-line portion of the dispersion characteristics over a wide frequency range. The dispersion shaping was projected for typically chosen TE₀₁-mode. The results were validated against those obtained for the conventional and un-conventional known structures and those obtained using commercially available simulation tool. The variation of azimuthal electric field intensity over the radial coordinate was also studied to examine the control of structure parameter for maxima-position, where the gyrating electron beam would be positioned for optimum beam-wave interaction in a gyro-TWT.

1. INTRODUCTION

The fantasy of periodic structures may be seen in antennas, antenna feeds, electromagnetic filters, phase shifters, polarizers, photonic

Received 28 May 2012, Accepted 30 July 2012, Scheduled 14 September 2012

* Corresponding author: Jaishanker Prasad Keshari (jaishanker_keshari@yahoo.co.in).

crystals for optical power dividers, multiplexers, switches, photonic band gap structures for solid-state lasers [1–10], etc. and even in the vacuum electronic devices, such as, linear/particle accelerators [11, 12], backward-wave oscillators (BWOs) [13], magnetrons [14], coupled-cavity and helix travelling-wave tubes (TWTs) [15–19], cyclotron masers [20, 21], gyrotron sources [21–24] and amplifiers [24–39], etc.. In these devices, one may see the periodic beam-wave interaction structures holding either azimuthal or axial periodicity [20–39]. The azimuthal periodicity in interaction structure may be seen, for example: in travelling-wave magnetrons [14] for π -mode operation, in gyrotrons [21–24] for mode rarefaction, in conventional helix-TWTs [17] for broadbanding, in gyro-travelling wave tubes (gyro-TWTs) [25, 26] for higher interaction impedance and, in turn, for higher device-gain. The axial periodicity in interaction structure may be seen, for example, in conventional helix-TWT [17] for higher device-gain, in coupled-cavity TWT [17] for getting fundamental-mode backward-wave characteristics, and in gyro-TWT [27–39] for broadbanding.

The axial-periodicity in the interaction structure of a gyro-TWT promises the broadbanding through dispersion shaping that allows wideband coalescence between the beam- and waveguide-mode dispersion characteristics and, in turn, the broadband gain-frequency response [27–37]. Choe and Uhm [36] analyzed the infinitesimally thin disc-loaded circular waveguide ignoring the higher order stationary- and propagating-wave modes in the field matching technique and presented the dispersion shaping by changing the structure parameters. Kesari et al. [27–30] improved the analysis of Choe and Uhm [26] considering higher order stationary- and propagating-wave modes, first for infinitesimally thin disc-loaded waveguide [27, 28] and then for thick disc-loaded waveguide [28–30]. Kesari [31, 32] also proposed the coaxial-disc-loaded circular waveguide interaction structure, such that in one configuration metal discs radially projecting inward from the metallic wall, and in second configuration metal discs radially projecting outward from the coaxial insert, for the beam-absent [31] and the beam-present [32] cases, and demonstrated the second configuration a better interaction structure. Yue et al. [33] also analyzed, in field matching technique, a coaxial circular waveguide with arbitrary shaped grooves on the wall, by profiling the groove in a series of rectangular steps [33].

A non-periodic continuous dielectric, in the form of wall-lining or coaxial rod, loaded circular waveguide also promises broadbanding of a gyro-TWT through dispersion shaping [40]. It holds the attenuator effects for self and parasitic oscillations, and brings the

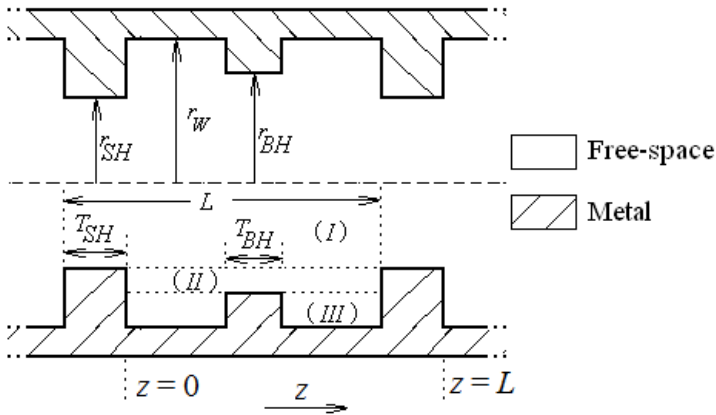


Figure 1. Cut-view of a disc-loaded circular waveguide of varying inner radii of alternate annular discs (structure under study).

problem of dielectric charging and associated heating, in case of lossy dielectrics [40]. Kesari et al. [34] combined the two methods, metal and dielectric loadings, of dispersion shaping to propose an alternatively metal and dielectric discs-loaded circular waveguide with same [34] and with different [35] metal and dielectric disc-hole radii. The dispersion characteristics of a similar structure in absence and in presence of annular electron beam were also analyzed in [13] including the instability performance.

In order to add an extra structure parameter in the promising disc-loaded circular waveguide and to examine the control of new parameter on the dispersion shaping, a new interaction structure is considered. This new structure is similar to a disc-loaded circular waveguide, in which the disc-hole radii of two consecutive discs are not same, however, the disc-hole radii of every second discs are same (Fig. 1). The paper consists of an analytical model and its analysis (Section 2), discussing electromagnetic boundary conditions (Section 2.1), and analytical steps to obtain the dispersion relation (Section 2.2) of the structure. A numerical code is developed for solving the dispersion relation and the roots are used to plot the dispersion characteristics and to see the control of structure parameters on dispersion shaping (Section 3).

2. ANALYTICAL MODEL AND ANALYSIS

The model of the structure considers a disc-loaded circular waveguide of varying inner radii of alternate discs (structure under study). The discs are organized in the circular waveguide such that the disc of the

bigger hole-radius is symmetrically in the middle of two alternate discs of the smaller hole-radii, and vice-versa. As the structure is periodic, therefore one period of the structure coupled with Floquet's theorem is sufficient for the analysis of an infinitely long structure. In the analytical model, one may divide the structure into three regions, such as: i) region *I*: $0 \leq r < r_{SH}$; ii) region *II*: $r_{SH} \leq r < r_{BH}$; and iii) region *III*: $r_{BH} \leq r < r_W$, where r_{SH} and r_{BH} are, respectively, the hole-radii of metal discs of smaller and bigger holes. r_W is the waveguide radius. One may take L as the axial periodicity of the structure, and T_{SH} and T_{BH} as the thicknesses of metal discs of smaller and bigger holes, respectively. Thus, one may calculate the axial-gap between two consecutive discs (which is the distance between discs of smaller and bigger hole-radii) as $(L - T_{SH} - T_{BH})/2$. Clearly, in the said model, one may consider, the region *I* (disc free region) supporting propagating and the regions *II* and *III* (disc occupied regions) supporting standing waves. The axial magnetic and azimuthal electric field intensities in various considered regions are, respectively [27–35]:

In region *I*:

$$H_z^I = \sum_{n=-\infty}^{+\infty} A_n^I J_0 \{ \gamma_n^I r \} \exp j (\omega t - \beta_n z) \quad (1)$$

$$E_\theta^I = j\omega\mu_0 \sum_{n=-\infty}^{+\infty} \frac{1}{\gamma_n^I} A_n^I J_0' \{ \gamma_n^I r \} \exp j (\omega t - \beta_n z) \quad (2)$$

In region *II*:

$$H_z^{II} = \sum_{m=1}^{\infty} [A_m^{II} J_0 \{ \gamma_m^{II} r \} + B_m^{II} Y_0 \{ \gamma_m^{II} r \}] \exp(j\omega t) \sin(\beta_m z) \quad (3)$$

$$E_\theta^{II} = j\omega\mu_0 \sum_{m=1}^{\infty} \frac{1}{\gamma_m^{II}} [A_m^{II} J_0' \{ \gamma_m^{II} r \} + B_m^{II} Y_0' \{ \gamma_m^{II} r \}] \exp(j\omega t) \sin(\beta_m z) \quad (4)$$

In region *III*:

$$H_z^{III} = \sum_{p=1}^{\infty} A_p^{III} Z_0 \{ \gamma_p^{III} r \} \exp(j\omega t) \sin(\beta_p z) \quad (5)$$

$$E_\theta^{III} = j\omega\mu_0 \sum_{p=1}^{\infty} \frac{1}{\gamma_p^{III}} A_p^{III} Z_0' \{ \gamma_p^{III} r \} \exp(j\omega t) \sin(\beta_p z), \quad (6)$$

where $Z_0 \{ \gamma_p^{III} r \} = J_0 \{ \gamma_p^{III} r \} Y_0' \{ \gamma_p^{III} r_W \} - J_0' \{ \gamma_p^{III} r_W \} Y_0 \{ \gamma_p^{III} r \}$; J_0 and Y_0 are the zeroth order Bessel functions of the first and second

kinds, respectively. Prime with a function represents its derivative with respect to its argument. $A_n^I, A_m^{II}, B_m^{II}$ and A_p^{III} are the field constants, superscript identifying its value, in different analytical regions. $\gamma_n^I [= (k^2 - \beta_n^2)^{1/2}]$, $\gamma_m^{II} [= (k^2 - \beta_m^2)^{1/2}]$, and $\gamma_p^{III} [= (k^2 - \beta_p^2)^{1/2}]$ are the radial propagation constants in regions *I*, *II*, and *III*, respectively. $\beta_n [= \beta_0 + 2\pi n/L]$ is the axial phase propagation constant in disc free region *I*; here, β_0 is the axial phase propagation constant for fundamental space harmonic, and $n [= 0, \pm 1, \pm 2, \pm 3, \dots]$ is space harmonic number. $\beta_m [= m\pi/(L - T_{SH})]$ (where $m = 1, 2, 3, \dots$) and $\beta_p [= 2p\pi/(L - T_{SH} - T_{BH})]$ (where $p = 1, 2, 3, \dots$) are the axial propagation constants in regions *II* and *III*, respectively; here m and p are the modal harmonic numbers in regions *II* and *III*, respectively.

2.1. Electromagnetic Boundary Conditions

One may write the relevant boundary conditions, stating the continuity of the tangential component of electric and the axial component of magnetic field intensities at the interface, $r = r_{BH}$, between the regions *II* and *III* (Fig. 1), as:

$$\left. \begin{aligned} E_\theta^{II} &= E_\theta^{III} & \text{(a)} \\ H_z^{II} &= H_z^{III} & \text{(b)} \end{aligned} \right\} 0 < z < (L - T_{SH} - T_{BH})/2 \quad (r = r_{BH}), \quad (7)$$

and stating the continuity of the tangential components of electric and the axial component of magnetic field intensities at the interface, $r = r_{SH}$, between the regions *I* and *II* (Fig. 1) as well as the vanishing tangential component of electric field intensity at the metal inner circumferential surface of the discs of smaller hole radii, $r = r_{SH}$, as:

$$E_\theta^I = \begin{cases} E_\theta^{II} & 0 < z < L - T_{SH} \\ 0 & L - T_{SH} \leq z \leq L \end{cases} \quad (r = r_{SH}), \quad (8)$$

$$H_z^I = H_z^{II} \quad 0 < z < L - T_{SH} \quad (r = r_{SH}). \quad (9)$$

2.2. Dispersion Relation

It is a usual practice in field matching technique to get the dispersion relation by substituting the field intensity components into the relevant boundary conditions and then eliminating the field constants. One may substitute the field expressions from (3)–(6) into (7(a)) and (7(b)), here for the sake of simplicity it is being considered that only one modal harmonic is present (say, m th in region *II* and p th in region *III*) in each of regions *II* and *III*, to represent B_m^{II} in terms of A_m^{II} while

eliminating A_p^{III} from the resulting relations, as:

$$\frac{B_m^{II}}{A_m^{II}} = \frac{\gamma_p^{III} J_0' \{ \gamma_m^{II} r_{BH} \} Z_0 \{ \gamma_p^{III} r_{BH} \} - \gamma_m^{II} J_0 \{ \gamma_m^{II} r_{BH} \} Z_0' \{ \gamma_p^{III} r_{BH} \}}{\gamma_m^{II} Y_0 \{ \gamma_m^{II} r_{BH} \} Z_0' \{ \gamma_p^{III} r_{BH} \} - \gamma_p^{III} Y_0' \{ \gamma_m^{II} r_{BH} \} Z_0 \{ \gamma_p^{III} r_{BH} \}}. \quad (10)$$

Further, the ratio B_m^{II}/A_m^{II} will be written as $\xi (= B_m^{II}/A_m^{II})$. Now, one may express the field constants A_m^{II} ($m = 1, 2, 3, \dots$), in terms of a series involving A_n^I ($-\infty < n < \infty$). For this purpose, one may substitute the field expressions (1) and (3), where in later B_m^{II} is represented in terms of A_m^{II} using (10), into (9), multiply it by $\sin(\beta_m^{II} z)$, then integrate it between $z = 0$ and $z = (L - T_{SH})$, to obtain:

$$A_m^{II} = \sum_{n=-\infty}^{\infty} A_n^I U_{nm}, \quad (11)$$

where

$$U_{nm} = \frac{2}{(L - T_{SH})} \frac{J_0 \{ \gamma_n^I r_{SH} \} \beta_m [1 - (-1)^m \exp(-j\beta_n(L - T_{SH}))]}{[J_0 \{ \gamma_m^{II} r_{SH} \} + \xi Y_0 \{ \gamma_m^{II} r_{SH} \}] (\beta_m^2 - \beta_n^2)}.$$

Similarly, one may obtain another series expression, similar to (11), for A_m^{II} ($m = 1, 2, 3, \dots$), but now with the help of the field expressions (2) and (4), instead of (1) and (3), respectively, and the boundary condition (8), instead of (9), and by changing the integration limits to $z = 0$ and $z = L$, instead of $z = 0$ and $z = (L - T_{SH})$, as follows:

$$A_m^{II} = \sum_{n=-\infty}^{\infty} A_n^I S_{nm}, \quad (12)$$

where

$$S_{nm} = \frac{2\gamma_m^{II} J_0' \{ \gamma_n^I r_{SH} \} [\beta_m - \exp(-j\beta_0 L) [\beta_m \cos(\beta_m L) + j\beta_n \sin(\beta_m L)]]}{\gamma_n^I [J_0' \{ \gamma_m^{II} r_{SH} \} + \xi Y_0' \{ \gamma_m^{II} r_{SH} \}] (\beta_m^2 - \beta_n^2) (L - T_{SH})}.$$

The following relation results by equating the right hand sides of (11) and (12):

$$\sum_{n=-\infty}^{\infty} A_n^I (U_{nm} - S_{nm}) = 0. \quad (13)$$

One can form v (say) number of simultaneous equations in the field constants A_n^I with the help of (13) while choosing v number of the stationary-wave modal number (m) as well as the space harmonic number (n), such as $n = 0, \pm 1, \pm 2, \pm 3$, and $m = 1, 2, 3, 4, 5, 6, 7$, for $v = 7$ (typically). Further, one may equate the determinant formed by the coefficients of the constants occurring in these equations to zero, as

the condition for the non-trivial solution of these equations, that would yield the following dispersion relation of the structure under study:

$$\det | M_{nm} J_0 \{ \gamma_n^I r_{SH} \} [J_0' \{ \gamma_m^{II} r_{SH} \} + \xi Y_0' \{ \gamma_m^{II} r_{SH} \}] - J_0' \{ \gamma_n^I r_{SH} \} [J_0 \{ \gamma_m^{II} r_{SH} \} + \xi Y_0 \{ \gamma_m^{II} r_{SH} \}] | = 0 \quad (-\infty < n < \infty, 1 \leq m < \infty), \quad (14)$$

where

$$M_{nm} = \frac{\gamma_n^I \beta_m [1 - (-1)^m \exp(-j\beta_n(L - T_{SH}))]}{\gamma_m^{II} [\beta_m - \exp(-j\beta_0 L) [\beta_m \cos(\beta_m L) + j\beta_n \sin(\beta_m L)]]}$$

3. RESULTS AND DISCUSSION

One may start validating the analytically obtained dispersion relation (14) with reference to the special cases of the structure: for the case, i) $r_{SH} \rightarrow r_W$ the dispersion relation (14) becomes the same, as that for the disc-loaded circular waveguide of disc-hole radius r_{BH} , disc-thickness T_{BH} , and periodicity L [28, 29]; ii) $r_{BH} \rightarrow r_W$, (14) becomes the same as that for the disc-loaded circular waveguide of disc-hole radius r_{SH} , disc-thickness T_{SH} , and periodicity L [28, 29]; iii) $r_{SH} = r_{BH}$ and $T_{SH} = T_{BH}$, (14) becomes as that for disc-loaded circular waveguide of disc-hole radius $r_{BH} (= r_{SH})$, disc-thickness $T_{BH} (= T_{SH})$, and periodicity $L/2$ [28, 29]; iv) $r_{SH} = r_{BH}$ and $T_{SH} + T_{BH} = L$, (14) becomes $J_0' \{ \gamma_n^I r_{SH} \} = J_0' \{ \gamma_n^I r_{BH} \} = 0$, which is dispersion relation of the smooth-wall circular waveguide of radius $r_{BH} (= r_{SH})$; and v) $r_{SH} = r_{BH} \rightarrow r_W$, (14) becomes $J_0' \{ \gamma_n^I r_W \} = 0$, which is dispersion relation of the smooth-wall circular waveguide of radius r_W . Also, while considering infinitesimally

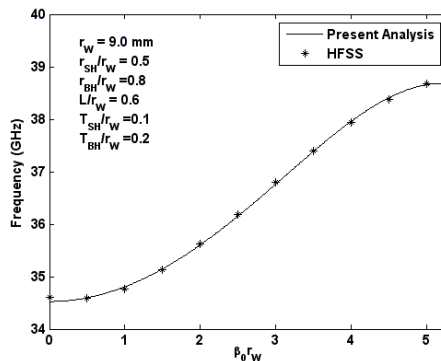


Figure 2. TE₀₁-mode dispersion characteristics of the structure under study obtained by present analysis (solid curve) in comparison/validation with that obtained using HFSS (asterisk symbols).

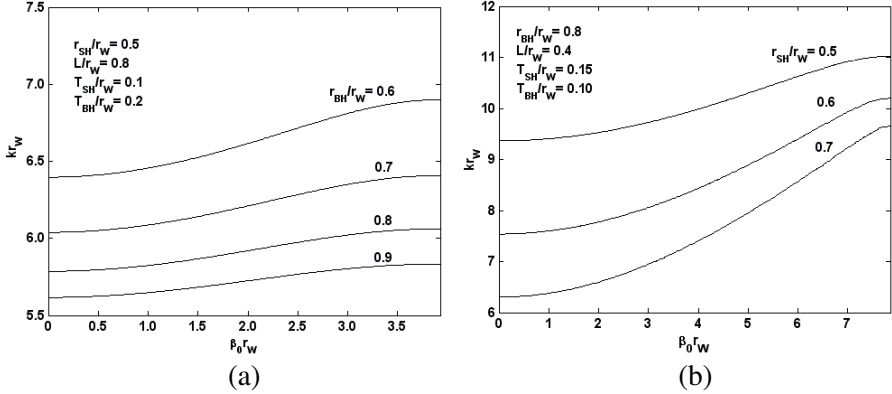


Figure 3. Dispersion characteristics of the structure under study, taking (a) bigger (r_{BH}/r_W) and (b) smaller (r_{SH}/r_W) hole-radii as the parameter.

thin disc, (14) passes to that published for infinitesimally thin disc-loaded circular waveguide [27, 28], and while ignoring the higher order harmonics passes to that published in [36]. All these cases are also validated with reference to the dispersion characteristics, obtained using the numerical code developed for solving the dispersion relation (14). In order to validate the dispersion characteristics obtained using the numerical code, a structure model, for typically chosen structure dimensions, is made in workspace of commercially available simulation tool — high frequency structure simulator (HFSS). The HFSS-model is analyzed using eigenmode solver and by observing the field-intensity pattern, the solutions for azimuthally symmetric TE modes are segregated and compared with the analytical results within 3% (Fig. 2). As expected, the structure due to its axial periodicity shows a periodic dispersion characteristics showing alternate stop- and pass-bands, pass-band lying between two consecutive frequency points of zero group velocities (Figs. 2–6).

The dispersion relation (14) is true for any azimuthally symmetric TE mode, however, one may choose the lowest order, i.e., TE₀₁-mode (typically), in order to show the potential of the structure under study for a gyro-TWT. (Further, the results are discussed for the TE₀₁-mode.) Similar to the conventional disc-loaded circular waveguide, both the hole-radii (bigger and smaller) of the structure under study are responsive to dispersion shaping. In general, the lower- and the upper-cutoff frequencies increase with decrease in hole-radii (Fig. 3), however, in particular, the passband increases (Fig. 3(a)) and decreases (Fig. 3(b)) with decrease of bigger and smaller hole-radii, respectively.

The disc-thickness of bigger-hole-disc is neither very responsive for dispersion shaping, nor for passband, however, the passband shifts to higher frequency side (Fig. 4(a)). One may use this nature for shifting the interaction band in order to achieve an optimum beam-wave interaction while designing a gyro-TWT with the structure under study. On the other hand, one may see an interesting phenomenon with the change of disc-thickness of smaller-hole-disc. The passband increases with increase as well as with decrease of disc-thickness of smaller-hole-disc with reference to that of bigger-hole-disc, in addition, the disc-thickness of smaller-hole-disc is also responsive for dispersion shaping (Fig. 4(b)).

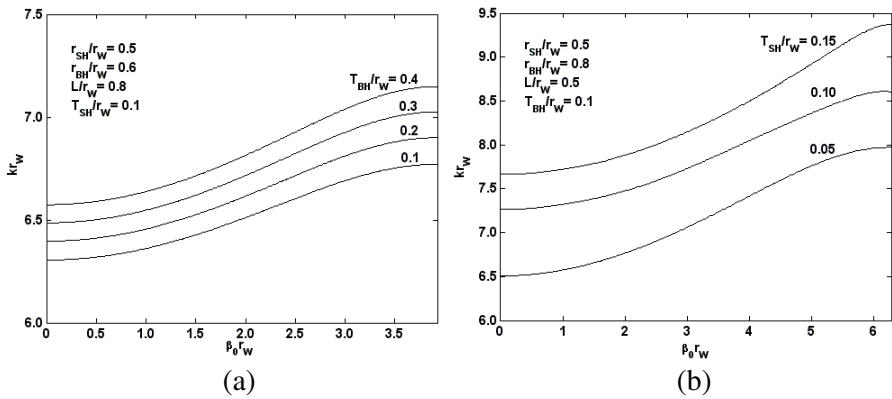


Figure 4. Dispersion characteristics of the structure under study, taking the disc-thickness of (a) bigger-hole-disc (T_{BH}/r_W) and (b) smaller-hole-disc (T_{SH}/r_W), as the parameter.

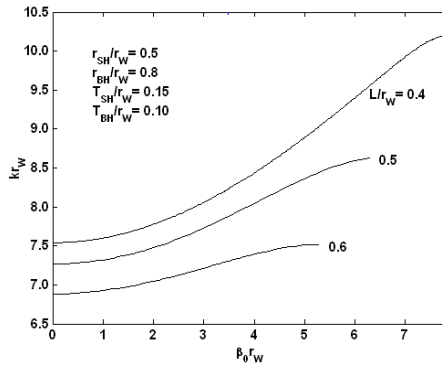


Figure 5. Dispersion characteristics of the structure under study, taking the structure periodicity (L/r_W), as the parameter.

The structure periodicity plays same way as that in case of conventional disc-loaded circular waveguide [28–30]. The structure periodicity is the most responsive for the passband as well as for dispersion shaping (Fig. 5), therefore, one may look forward to the periodicity of the structure under study for achieving a broadband coalescence between beam- and waveguide-mode dispersion characteristics while designing the device. While finding the straight-line portion of the dispersion characteristics of the structure, which is required for broadband coalescence with beam-mode dispersion line, one may plot the slope of the dispersion ($\omega - \beta$) characteristics, which generally gives the group-velocity (v_g/c), verses frequency (Fig. 6). In the plot, for the broadband performance, one may look for region of constant group-velocity, which is basically reflection of straight-line portion of the dispersion characteristics. The peak of the curve thus generated would typically correspond to axial beam velocity required for beam-wave synchronism. While examining Fig. 6, one may find the results for the disc-loaded circular waveguides of constant disc-hole radii at two extreme ends. Here, it is necessary to point out that the disc-loaded circular waveguides presented at two extreme ends differs in periodicity. However, leaving the right-most broken curve apart, all other curves correspond to same periodicity. One may observe the increase in region of constant group-velocity with decrease in bigger hole-radius, however, with shift of the frequency band (Fig. 6). The corresponding shift of the frequency band may be compensated with change in either waveguide radius or disc-thickness of bigger-hole-disc or both. Therefore, as expected, the structure under study adds an extra structure parameter in the promising disc-loaded circular waveguide, and also the new parameter helps in dispersion shaping.

In addition to assess the structure for broadbanding a gyro-TWT, it is also important to examine the radial position of maximum azimuthal electric field intensity where the gyrating electron beam is located for optimum beam-wave interaction. For this examination, one has to first substitute the solutions of the dispersion relation (14) into the azimuthal electric field intensity component (2) for $0 \leq r < r_{SH}$, (4) for $r_{SH} \leq r < r_{BH}$, and (6) $r_{BH} \leq r < r_W$, respectively, in regions *I*, *II* and *III*; and, secondly, while selecting the solution of the dispersion relation, one has to choose $\beta_0 \approx 0$, that correspond to the cut-off frequency of interaction structure where a gyro-TWT operates, in order to reduce the effect of beam-velocity spread and pulse distortion. It is interesting to note that the change in structure parameters not only shapes the dispersion characteristics and controls the passband, but also controls the position of maximum azimuthal

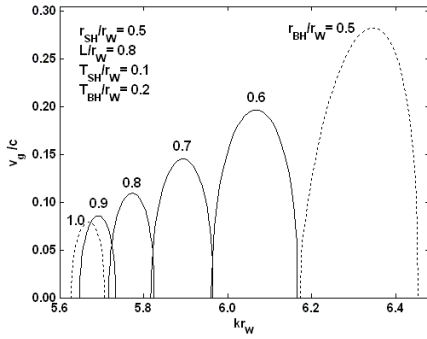


Figure 6. Normalized group-velocity versus normalized frequency characteristics of the structure under study, taking bigger hole-radius (r_{BH}/r_W) as the parameter. Special cases leading to disc-loaded circular waveguide of constant disc-hole radius (broken curve).

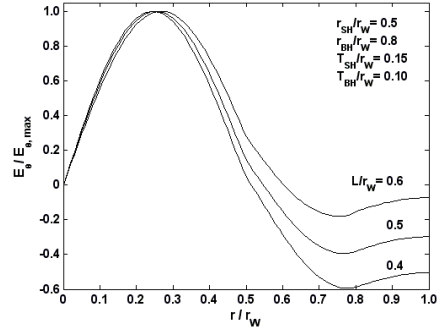


Figure 7. Azimuthal electric field intensity variation over the radial coordinate in the structure under study, taking the structure periodicity (L/r_W), as the parameter.

electric field intensity for positioning of the gyrating electron beam (Fig. 7). It has been observed that with increase of structure-periodicity the position of maximum azimuthal electric field intensity shifts away from the axis (Fig. 7). It is obvious that as the discs come closer, the electric field available between the discs decreases and the field strength increases in the disc free region radially away from disc, and in turn accordingly the shift of azimuthal electric field maxima occur.

In an overview, the approximation used while eliminating the field constants, in particular, while calculating $\xi (= B_m^{II}/A_m^{II})$ makes the analysis as well as the numerical program simple. (Here, m and p are considered as 1 for lowest order modal harmonics.) However, in addition, a rigorous analysis is tried considering numbers of m and p values in boundary condition (7) and averaging the field values over the axial limit between the two consecutive discs of smaller hole-radii. The rigor of the analysis for B_m^{II}/A_m^{II} converges to the value very close to that obtained using (10), and also the results obtained by presented analysis (Section 2) are validated against those obtained using HFSS. Therefore, instead of rigorous analysis, which makes the dispersion relation bulky and takes the computational time ~ 10 to 15 times more than that of simple analysis, the simple analysis is presented.

4. CONCLUSION

The authors have proposed a novel interaction structure, which is a disc-loaded circular waveguide of varying inner radii of alternate discs, for a wideband gyro-TWT. The structure periodicity and the disc-thickness of bigger-hole-disc are, respectively, the most and the least responsive for the passband as well as for dispersion shaping. In addition to dispersion shaping, which is required for designing a broadband gyro-TWT, the structure also holds a fascinating characteristic of increase in passband with increase as well as with decrease of disc-thickness of smaller-hole-disc with reference to that of bigger-hole-disc. The passband improvement can be achieved by varying the disc radii for a given beam-mode dispersion characteristic. In the present manuscript, only the dispersion analysis has been presented in absence of gyrating electron-beam, however, the authors are aware that the broadbanding may be better seen in gain-frequency response obtained in the beam present small signal analysis, as has been done earlier by authors.

REFERENCES

1. Lin, H.-N. and C.-C. Tang, "Analysis and design for high-gain antenna with periodic structures," *PIERS Online*, Vol. 6, No. 2, 181–184, 2010.
2. Dehdasht-Heydari, R., H. R. Hassani, and A. R. Mallahzadeh, "A new 2–18 GHz quad-ridged horn antenna," *Progress In Electromagnetics Research*, Vol. 81, 183–195, 2008.
3. Dai, G. L. and M. Y. Xia, "Novel miniaturized bandpass filters using spiral-shaped resonators and window feed structures," *Progress In Electromagnetics Research*, Vol. 100, 235–243, 2010.
4. Yang, M. H., J. Xu, Q. Zhao, L. Peng, and G. P. Li, "Compact, broad-stopband lowpass filters using sirs-loaded circular hairpin resonators," *Progress In Electromagnetics Research*, Vol. 102, 95–106, 2010.
5. Chiou, Y.-C., P.-S. Yang, J.-T. Kuo, and C.-Y. Wu, "Transmission zero design graph for dual-mode dual-band filter with periodic stepped-impedance ring resonator," *Progress In Electromagnetics Research*, Vol. 108, 23–36, 2010.
6. Butt, H., Q. Dai, T. D. Wilkinson, and G. A. J. Amaratunga, "Photonic crystals & metamaterial filters based on 2D arrays of silicon nanopillars," *Progress In Electromagnetics Research*, Vol. 113, 179–194, 2011.

7. Wu, C.-J., Y.-H. Chung, B.-J. Syu, and T.-J. Yang, "Band gap extension in a one-dimensional ternary metal-dielectric photonic crystal," *Progress In Electromagnetics Research*, Vol. 102, 81–93, 2010.
8. Xie, H.-H., Y.-C. Jiao, K. Song, and Z. Zhang, "A novel multi-band electromagnetic band-gap structure," *Progress In Electromagnetics Research Letters*, Vol. 9, 67–74, 2009.
9. Jandieri, V., K. Yasumoto, and Y.-K. Cho, "Rigorous analysis of electromagnetic scattering by cylindrical EBG structures," *Progress In Electromagnetics Research*, Vol. 121, 317–342, 2011.
10. Escorcía-García, J. and M. E. Mora-Ramos, "Study of optical propagation in hybrid periodic/quasiregular structures based on porous silicon," *PIERS Online*, Vol. 5, No. 2, 167–170, 2009.
11. Wei, S., Y. Lin, and T. Higo, "A new method for dispersion curves of HOM in periodical axisymmetric accelerating structures," *Proc. 2nd Asian Particle Accelerator Conf.*, 153–155, Beijing, China, 2001.
12. Hu, Y., C. Tang, H. Chen, Y. Lin, and D. Tong, "An X-band disk and washer accelerating structure for electron accelerators," *Proc. Particle Accelerator Conf.*, 975–977, Chicago, 2001.
13. Amin, M. R. and K. Ogura, "Dispersion characteristics of a rectangularly corrugated cylindrical slow-wave structure driven by a non-relativistic annular electron beam," *IET Microwave Antennas Propag.*, Vol. 1, No. 3, 575–579, 2007.
14. Ding, S., B. Jia, F. Li, and Z. Zhu, "3D Simulation of 18-vane 5.8 GHz magnetron," *Journal of Electromagnetic Waves and Applications*, Vol. 22, Nos. 14–15, 1925–1930, 2008.
15. Malek, F., "The analytical design of a folded waveguide traveling wave tube and small signal gain analysis using Madey's theorem," *Progress In Electromagnetics Research*, Vol. 98, 137–162, 2009.
16. Mulcahy, T., H. Song, and F. Francisco, "New method of integrating periodic permanent magnet (PPM) assembly in traveling wave tubes (TWTs)," *Progress In Electromagnetics Research C*, Vol. 10, 187–199, 2009.
17. Jain, P. K. and B. N. Basu, "Electromagnetic wave propagation through helical structures," *Electromagnetic Fields in Unconventional Materials*, O. N. Singh and A. Lakhtakia, Ed., John Wiley & Sons, USA, 2000.
18. Hou, Y., J. Xu, H.-R. Yin, Y.-Y. Wei, L.-N. Yue, G. Zhao, and Y.-B. Gong, "Equivalent circuit analysis of ridge-loaded folded-waveguide slow-wave structures for millimeter-wave traveling-

- wave tubes,” *Progress In Electromagnetics Research*, Vol. 129, 215–229, 2012.
19. Liu, Y., J. Xu, Y.-Y. Wei, X. Xu, F. Shen, M. Huang, T. Tang, W.-X. Wang, Y.-B. Gong, and J. Feng, “Design of a V-band high-power sheet-beam coupled-cavity traveling-wave tube,” *Progress In Electromagnetics Research*, Vol. 123, 31–45, 2012.
 20. Jerby, E. and G. Bekefi, “Cyclotron maser experiments in a periodic wave guide,” *Phys. Rev. E*, Vol. 48, No. 6, 4637–4641, 1993.
 21. Chu, K. R., “The electron cyclotron maser,” *Rev. Mod. Phys.*, Vol. 76, No. 2, 489–540, May 2004.
 22. Barroso, J. J., R. A. Correa, and P. J. de Castro, “Gyrotron coaxial cylindrical resonators with corrugated inner conductor: Theory and experiment,” *IEEE Trans. on Microwave Theory and Tech.*, Vol. 46, No. 9, 1221–1230, Sep. 1998.
 23. Zaginaylov, G. I. and I. V. Mitina, “Electromagnetic analysis of coaxial gyrotron cavity with the inner conductor having corrugations of an arbitrary shape,” *Progress In Electromagnetics Research B*, Vol. 31, 339–356, 2011.
 24. Thumm, M., “State-of-the-art of high-power gyro-devices and free electron masers, update 2011,” Scientific Report KITSR 7606, Karlsruhe Institute of Technology, Germany, Jan. 2012.
 25. Singh, G., “Analytical study of the interaction structure of vane-loaded gyro-traveling wave tube amplifier,” *Progress In Electromagnetics Research B*, Vol. 4, 41–66, 2008.
 26. Qiu, C. R., Z. B. Ouyang, S. C. Zhang, H. B. Zhang, and J. B. Jin, “Self-consistent nonlinear investigation of an outer-slotted-coaxial waveguide gyrotron traveling-wave amplifier,” *IEEE Trans. on Plasma Sci.*, Vol. 33, No. 3, 1013–1018, Jun. 2005.
 27. Kesari, V., P. K. Jain, and B. N. Basu, “Analytical approaches to a disc loaded cylindrical waveguide for potential application in wideband gyro-TWTs,” *IEEE Trans. on Plasma Sci.*, Vol. 32, No. 5, 2144–2151, Oct. 2004.
 28. Kesari, V., *Analysis of Disc-loaded Circular Waveguides for Wideband Gyro-TWTs*, LAP — Lambert Academic Publishing AG & Co., Germany, 2009, (ISBN: 978-3-8383-1145-6).
 29. Kesari, V., P. K. Jain, and B. N. Basu, “Analysis of a circular waveguide loaded with thick annular metal discs for wideband gyro-TWTs,” *IEEE Trans. on Plasma Sci.*, Vol. 33, No. 4, 1358–1365, Aug. 2005.
 30. Kesari, V., P. K. Jain, and B. N. Basu, “Analysis of a disc-

- loaded circular waveguide for interaction impedance of a gyrotron amplifier,” *Int. J. Infrared and Millimeter Waves*, Vol. 26, No. 8, 1093–1110, Aug. 2005.
31. Kesari, V., “Beam-absent analysis of disc-loaded-coaxial waveguide for its application in gyro-TWT (Part-1),” *Progress In Electromagnetic Research*, Vol. 109, 211–227, 2010.
 32. Kesari, V., “Beam-present analysis of disc-loaded-coaxial waveguide for its application in gyro-TWT (Part-2),” *Progress In Electromagnetic Research*, Vol. 109, 229–243, 2010.
 33. Yue, L., W. Wang, Y. Wei, and Y. Gong, “Approach to a coaxial arbitrary-shaped groove cylindrical waveguide for application in wideband gyro-TWTs,” *IEEE Trans. on Plasma Sci.*, Vol. 35, No. 3, 551–558, Jun. 2007.
 34. Kesari, V., P. K. Jain, and B. N. Basu, “Modeling of axially periodic circular waveguide with combined dielectric and metal loading,” *J. Physics D: Applied Physics*, Vol. 38, 3523–3529, Sep. 2005.
 35. Kesari, V. and J. P. Keshari, “Analysis of a circular waveguide loaded with dielectric and metal discs,” *Progress In Electromagnetic Research*, Vol. 111, 253–269, 2011.
 36. Choe, J. Y. and H. S. Uhm, “Theory of gyrotron amplifiers in disc or helix loaded waveguides,” *Int. J. Electron.*, Vol. 53, No. 6, 729–741, Jun. 1982.
 37. Leou, K. C., T. Pi, D. B. Mcdermott, and N. C. Luhmann, Jr., “Circuit design for a wideband disc loaded gyro-TWT amplifier,” *IEEE Trans. on Plasma Sci.*, Vol. 26, No. 3, 488–495, Jun. 1998.
 38. Denisov, G. G., V. L. Bratman, A. W. Cross, W. He, A. D. R. Phelps, K. Ronald, S. V. Samsonov, and C. G. Whyte, “Gyrotron traveling wave amplifier with a helical interaction waveguide,” *Phys. Rev. Lett.*, Vol. 81, No. 25, 5680–5683, Dec. 1998.
 39. Rao, S. J., P. K. Jain, and B. N. Basu, “Hybrid-mode helix-loading effects on gyro-travelling-wave tubes,” *Int. J. Electron.*, Vol. 82, No. 6, 663–675, Jun. 1997.
 40. Rao, S. J., P. K. Jain, and B. N. Basu, “Broadbanding of gyro-TWT by dielectric-loading through dispersion shaping,” *IEEE Trans. on Electron Dev.*, Vol. 43, No. 12, 2290–2299, Dec. 1996.